Exp Brain Res (2009) 196:497–509
DOI 10.1007/s00221-009-1878-2

RESEARCH ARTICLE

Trajectory of the index finger during grasping

Jason Friedman · Tamar Flash

Received: 15 September 2008 / Accepted: 21 May 2009 / Published online: 12 June 2009

Abstract The trajectory of the index finger during grasping movements was compared to the trajectories predicted by three optimization-based models. The three models consisted of minimizing the integral of the weighted squared joint derivatives along the path (inertia-like cost), minimizing torque change, and minimizing angular jerk. Of the three models, it was observed that the path of the fingertip and the joint trajectories, were best described by the minimum angular jerk model. This model, which does not take into account the dynamics of the finger, performed equally well when the inertia of the finger was altered by adding a 20 g weight to the medial phalange. Thus, for the finger, it appears that trajectories are planned based primarily on kinematic considerations at a joint level.

Keywords Finger · Kinematics · Trajectory · Grasping

Introduction

The present work examines the trajectory of the index finger during grasping movements, in particular, which endpoint paths and joint angle trajectories are used during these movements. Different models in the literature are compared based on their ability to describe the observed experimental data.

The study of grasping movements in humans has been mostly addressed from the perspective of reach-to-grasp movements, which have been typically considered as consisting of two independent components (Jeannerod 1981), one for bringing the hand to the location of the object, and the other for shaping the hand for the grasp. The focus of this article is on the component responsible for shaping the fingers during the grasp.

The major approach used in modeling this problem has been to specify the desired final joint configuration (Berkinblit et al. 1986), and to reach it in some way. The joints may move in a coordinated way (Rosenbaum et al. 2001; Dejmal and Zacksenhouse 2006), such that all the joint velocities are linearly related. This approach is supported by Principal Component Analysis (Santello et al. 2002) and singular value decomposition (Mason et al. 2001) of grasping movements, which show that a linear combination of joint velocities can account for most of the variance observed in finger movements. The velocity profiles of the joints are generally assumed to be bell shaped (Rosenbaum et al. 2001), which is approximately equivalent to minimizing angular jerk.

An alternative approach is to plan the movement of the fingertip, for example by minimizing jerk in Cartesian coordinates (Secco et al. 2004), which results in straight line fingertip trajectories. A similar idea is described in Smeets and Brenner (1999), however in that work, they have modeled the combined movement of the arm and the grasping fingers as following a minimum jerk trajectory, and by relaxing some constraints of the minimum jerk model, they were able to generate curved fingertip paths.

In modeling arm movements, energetic considerations have been the motivation for a number of models,

J. Friedman · T. Flash
Department of Computer Science and Applied Mathematics,
Weizmann Institute of Science, Rehovot, Israel

Present Address:
J. Friedman (✉)
Macquarie Centre for Cognitive Science,
Macquarie University, Sydney, Australia
e-mail: write.to.jason@gmail.com

including minimizing cost functions related to kinetic energy (Soechting et al. 1995; Biess et al. 2007) and torque change (Uno et al. 1989). In this work, such cost functions will be applied for modeling movements of the finger.

Empirical observations in the hand surgery literature have noted that the path taken by the fingertip approximately follows a logarithmic spiral (Littler 1973). Gupta et al. (1998) performed measurements of the paths taken by the fingers using a motion capture system and confirmed this finding, although they did not test any alternative parameterizations of the path. Recently, the index finger was measured during grasping, and the fingertips paths were fitted well by logarithmic spirals (Kamper et al. 2003), and better than the fit provided by parabolas.

In this work, three optimization-based models for how the central nervous system (CNS) may plan finger movements are presented and their predictions, given the initial and final postures during grasping movements, are compared. These models are based on minimizing an inertia-like cost, minimizing the rate of change of joint torques, and minimizing angular jerk. The finger movements will be assessed in two conditions—one with the finger moving in a regular fashion, and another one involving the addition of a weight to the medial phalange in order to significantly change the finger's inertial properties. Based on similar models for the arm (Biess et al. 2007), we have expected that an inertia-like cost function will produce predictions that are the closest match to the experimental data.

Materials and methods

The experimental data used here were taken from four of the subjects of the grasping experiments described in Friedman and Flash (2007). In this work, the subjects were required to grasp three different objects using only pad opposition grasps (i.e., grasps that only contact with the fingertips). They used two different grasps of each object, namely, lifting a cup from the top and from the side, unscrewing and lifting the lid of a narrow jar, and stirring with and lifting a teaspoon. In each trial, the subjects began with their hand at a marked position resting on the table, then after hearing a beep, they moved their hand to grasp the object, which they held until hearing a second beep, 2.5 s later. Following this phase, the subject manipulated the object as instructed for 2 s, after which he or she returned the object to its starting position. Each grasp was repeated three times. The angular rotations of the fingers were recorded using the CyberGlove (Immersion). The finger tip location during the movement was calculated from the joint angles using forward kinematics. The calibration parameters were individually defined for each subject.

During a typical grasping movement, the fingers first open, before closing in on the object (Jeannerod 1981). The part of the movement that is examined here is from the time of maximum aperture of the fingers to when the fingers grasp the object. The segmentation was performed by selecting the last continuous time segment before contact with the object where the three joint velocities being considered are all positive, i.e., the finger is closing on the object. The movement was considered to have been finished when the mean square finger joint velocities were below a threshold of 0.10 $rad^2\ s^{-2}$. Only grasping movements which started from rest (at the moment of maximum aperture) and the ones which had an arc length longer than 3 cm were considered. Shorter movements were not considered because such movements have paths very similar to a straight line, and thus it is difficult to differentiate between the predictions of the different models.

The lengths and radii of the fingers were measured using calipers. The mass was estimated by assuming that the phalanges are cylinders, with a density of 1,200 $kg\ m^{-3}$ (Dempster 1955). These data were used in calculating the inertia matrices for the fingers. The effect of using different values for these parameters was considered by calculating the sensitivity of the model predictions to variations in these parameters.

If the finger trajectories selected are indeed a result of energetic considerations, then changes in these trajectories should be observed if the inertia of the finger is changed. In order to test this possibility, the experiments from Friedman and Flash (2007) were repeated at a later time for the same four subjects analyzed in that paper, and examined with the addition of a weight of 20 g to the medial phalange of the index finger. This weight was in the form of a lead spiral, worn symmetrically around the phalange such that the inertia of the phalange would increase in a uniform way in all directions. This weight was much larger than the typical mass of this phalange (around 3 g). The lead spiral was sufficiently small that it could be worn inside the CyberGlove, and did not significantly affect their ability to move the finger. The subjects were given several minutes to make natural hand movements while wearing the coil (i.e., not those movements required for the task) to become familiar with wearing it, and were able to perform prehension tasks with no noticeable difficulties.

Parameterization of path by arc length

If the path of the fingertip was to follow a minimum jerk solution (Flash and Hogan 1985), where the integral of the squared sum of the jerk in Cartesian coordinates is minimized, the fingertip must follow a straight line, which clearly it does not. In the work of Kamper et al. (2003), it

was shown that even if the endpoint constraint that the acceleration be zero at the start and end of the movement is removed, the trajectory still does not minimize the jerk cost for the fingertip.

However, an alternative approach is to consider minimizing jerk on the Euclidean arc length (Biess et al. 2007), i.e., that the squared arc length jerk cost

$$C = \int_{t=0}^{t_f} \dddot{s}^2 \mathrm{d}t \tag{1}$$

is minimized along the specified path. The arc length is the length along the curve, and can be calculated by

$$s = \int_{\lambda=0}^{1} \sqrt{x'(\lambda)^2 + y'(\lambda)^2}\mathrm{d}\lambda \tag{2}$$

where λ is a variable that monotonically increases with the progression of the movement (such as time).

Models

To predict the trajectories of the index finger three different models were compared. As this work studied ecological grasping movements and strict instructions were not given regarding the starting and final postures during the grasping movement, the initial and final postures of the hand generally differed even between task repetitions by the same subject. Thus, when we refer to "predicting" the trajectory of the finger during grasping movements, we refer to predicting the time-varying joint angles and endpoint positions, of each individual movement, given the initial and final postures of the finger and the duration of the movement. Given these inputs, we determine the parameters of the models based on the given optimality criteria, but the predictions of the trajectories, based on the different models, do not in any way use any other details regarding the trajectories, as would be the case if using regression to find the best fit curve.

Numerous studies in the motor control literature have suggested various optimization-based models as a way of modeling how the CNS may select movements. In this work, we considered three models that have been successfully used previously to describe natural arm movements, and that could potentially describe the curved paths observed here. We selected two models which are based on energetic considerations and a third model which is based only on the optimization of a kinematic quantity (minimization of a joint jerk cost) to try to help elucidating the importance of energetic considerations during stereotypical finger movements used during grasping.

Inertia-like model

For the first model, the path and time course were selected independently, based on the assumption that separate planning constraints may be applied at the geometric and temporal levels, before being integrated into a complete representation (Biess et al. 2007). The path was selected to minimize the integral of the weighted squared joint derivatives along the path, in a similar way to the technique presented in Biess et al. (2007). The kinetic energy E_k of a multiple link open-chain manipulator like the finger can be written in terms of the manipulator inertia matrix (Murray et al. 1994):

$$E_k(\theta, \dot{\theta}) = \frac{1}{2}\dot{\theta}^T M(\theta)\dot{\theta} \tag{3}$$

where the 3×3 matrix M is known as the manipulator inertia matrix. The derivation of M for this model of the finger is described in "Appendix". The cost function used here is similar to the one expressed above, but the parameter is an arbitrary one (λ), rather than time, because it is assumed that the geometry is planned independently of the time course. The arbitrary parameter λ equals zero at the start of the path, 1 at the end of the path, and monotonically increases along the path. However, it is generally not linearly related to either time or arc length. Thus, the cost function is analogous but not equal to kinetic energy.

The definition is given by

$$C_E = \frac{1}{2}\int_{\lambda=0}^{1} \dot{\theta}(\lambda)^T M(\theta(\lambda))\dot{\theta}(\lambda)\mathrm{d}\lambda \tag{4}$$

These paths are geodesic in configuration space with respect to the above metric.

The direct minimization of kinetic energy is not suitable for finger movements, because it would result in a movement with constant velocity, which is inconsistent with the observed boundary conditions in natural point-to-point movements of zero joint velocity and acceleration at the start and end of the movement. However, the geodesics produced by minimization of the cost function in Eq. 4 have some attractive properties. Namely, the dynamics of the movement are simplified along these paths, as the terms due to the centrifugal and Coriolis forces disappear (Biess et al. 2007). It is only along paths minimizing this cost function that all the force can be used for accelerating along the path. This property is true regardless of the selected velocity profile.

The joint angles of the metacarpophalangeal (θ_{MPJ}) and proximal interphalangeal (θ_{PIJ}) joints were modeled using Jacobi polynomials (Wada et al. 2001; Biess et al. 2006). Complete details of the technique used can be found in

Biess et al. (2006). Each joint was modeled as a function of a parameter λ by

$$\theta(\lambda) = \theta_0 + (\theta_f - \theta_0)\lambda + \sum_{k=0}^{N} c_{ik}\varphi_k^{(1)}(\lambda), \quad 0 \le \lambda \le 1 \tag{5}$$

The first two terms here, which describe a straight line from the initial to the final joint angles, ensure that the boundary conditions are met. The basis functions, $\varphi_k^{(m)}(\lambda)$, are described in terms of Jacobi polynomials. Each basis function satisfies homogeneous boundary conditions. The basis functions are defined as (Wada et al. 2001; Biess et al. 2006)

$$\varphi_k^{(m)}(\lambda) = C_{k,m}2^{2m}\lambda^m(1-\lambda)^m P_k^{(2m,2m)}(2\lambda - 1) \tag{6}$$

where m is the order of the highest derivative in the cost functional, $C_{k,m}$ is a normalization factor, the term $\lambda^m(1-\lambda)^m$ ensures that the basis function vanishes at the boundary points, and $P_k^{(2m,2m)}$ is the Jacobi polynomial, defined by

$$P_n^{(\alpha,\beta)}(x) = \frac{1}{2^n}\sum_{k=0}^{n}\binom{n+\alpha}{k}\binom{n+\beta}{n-k}(x-1)^{n-k}(x+1)^k \tag{7}$$

Jacobi polynomials are used because they define a set of orthogonal functions on [0,1], while satisfying the correct boundary conditions. This means that using a sufficiently large number of polynomials, any (smooth) trajectory of θ can be captured (in the least squared sense). First, the value of c_{i0} was determined by minimizing the cost function using only the 0th order expansion. This value of c_{i0} was then fixed, and the process repeated for c_{i1} using the first-order expansion, and so on. The optimization was performed using nonlinear optimization, using the optimization toolkit in Matlab. In practice, only the first three polynomials were used because the coefficients became very small after this. The value of the cost function was evaluated at 1,000 steps of λ.

The time course was then set such that the squared jerk of the Euclidean arc length along the path (Eq. 1) was minimized. The optimal arc length jerk trajectory can be written as

$$\begin{aligned} s(t_n) &= s(1)\left(6t_n^5 - 15t_n^4 + 10t_n^3\right), \quad s(0) = 0, \\ t_n &= (t - t_0)/(t_f - t_0) \end{aligned} \tag{8}$$

The arc length at each sample point during the modeled movement was calculated using Eq. 2, and the movement was then resampled so that the arc length jerk would be minimized.

An outcome of using the minimum arc length jerk cost along these geodesic paths is that the peak kinetic energy is also minimized (Biess et al. 2007).

Minimum torque change

The second model used was the minimum torque-change model (Uno et al. 1989), which was used to predict the path and the time course.

The cost function used for the minimum torque-change model was

$$C_\tau = \frac{1}{2}\int \left(\frac{\mathrm{d}\tau(\theta)}{\mathrm{d}t}\right)^{\mathrm{T}}\left(\frac{\mathrm{d}\tau(\theta)}{\mathrm{d}t}\right)\mathrm{d}t \tag{9}$$

The torque is calculated using the inertia and Coriolis terms of the dynamic equation:

$$\tau = M(\theta)\ddot{\theta} + C(\theta,\dot{\theta})\dot{\theta} \tag{10}$$

The effects of gravity are neglected.

For this model, Jacobi polynomials were also used:

$$\begin{aligned} \theta(t_n) = \theta_0 + (\theta_f - \theta_0)\left(6t_n^5 - 15t_n^4 + 10t_n^3\right) \\ + \sum_{k=0}^{N} c_{ik}\varphi_k^{(3)}(t_n), \quad 0 \le t_n \le 1 \end{aligned} \tag{11}$$

where the coefficients c_{ik} were selected to minimize the cost. In this case, the first two terms describe a polynomial that satisfies the boundary conditions of the minimum torque-change model, namely, that the velocities and accelerations at the start and end are zero, as described in Nakano et al. (1999). For this model, the joint angles are modeled as a function of normalized time $t_n = t/t_f$, because the path and velocity profiles cannot be derived independently as with the previous model. In this case, the Jacobi polynomials are constructed with a basis where $m = 3$, corresponding to an expansion scheme of order $m = 3$.

Minimum angular jerk

The third model was the minimum angular jerk model (Okadome and Honda 1999; Hermens and Gielen 2004), which was used to predict both the path and the time course. That is, each joint will have a trajectory determined by

$$\begin{aligned} \theta(t_n) &= \theta_0 + (\theta_f - \theta_0)\left(6t_n^5 - 15t_n^4 + 10t_n^3\right), \\ t_n &= \frac{t - t_0}{t_f - t_0} \quad 0 \le t_n \le 1 \end{aligned} \tag{12}$$

This implies that there is a linear relationship between the metacarpophalangeal joint and the proximal interphalangeal joint, since both have the same time course.

This model does not require the use of optimization to determine the finger trajectory because the coefficients of the minimum jerk trajectory are known.

For all the models, the distal interphalangeal joint (θ_{DIJ}) was assumed to be determined by the proximal

interphalangeal joint, based on the findings of previous papers (Hahn et al. 1995). For each movement, the relationship between θ_{PIJ} and θ_{DIJ} was modeled by a third-order polynomial:

$$\theta_{\mathrm{PIJ}} = \mathrm{p}_1\theta_{\mathrm{DIJ}}^3 + \mathrm{p}_2\theta_{\mathrm{DIJ}}^2 + \mathrm{p}_3\theta_{\mathrm{DIJ}} + \mathrm{p}_4 \quad (13)$$

This was used, rather than a linear relationship as was suggested in Hahn et al. (1995), because at the extremes of the joint range, the linear relationship was found not to hold.

The minimization of the cost functions was performed in Matlab, using the non-linear optimization function in the Optimization toolkit. The torque for all the movements was estimated using Eq. 10.

Quality of fit

The quality of the predictions was compared by calculating the root mean square error (RMSE) between the predictions and the experimental data for Cartesian (xy) endpoint data E_{xy} with respect to the normalized arc length σ, and for the Cartesian endpoint velocities E_{vel} and joint angles E_{posture} with respect to normalized time:

$$E_{xy} = \sqrt{\frac{1}{N}\sum_{i=1}^{N}\left(x_e(\sigma_i) - x_p(\sigma_i)\right)^2 + \left(y_e(\sigma_i) - y_p(\sigma_i)\right)^2}$$

$$E_{\mathrm{vel}} = \sqrt{\frac{1}{N}\sum_{i=1}^{N}\left(\dot{x}_e(t_i) - \dot{x}_p(t_i)\right)^2 + \left(\dot{y}_e(t_i) - \dot{y}_p(t_i)\right)^2}$$

$$E_{\theta_k} = \sqrt{\frac{1}{N}\sum_{i=1}^{N}\left(\theta_{ke}(t_i) - \theta_{kp}(t_i)\right)^2}$$

$$E_{\mathrm{posture}} = E_{\theta_{\mathrm{MPJ}}} + E_{\theta_{\mathrm{PIJ}}} + E_{\theta_{\mathrm{DIJ}}} \quad (14)$$

The subscript p denotes the prediction of the model, and e the experimentally recorded data. The error in terms of the posture (joint angles) was calculated by summing the errors over the angles.

The first error measure considers differences only in the endpoint paths, whereas the second measure also considers the velocity profiles. The third error measure captures the differences in the joint angle trajectories with respect to time.

The errors of the different models in terms of the RMSE for the path, Cartesian endpoint velocity, and joint angle data were compared using multiple t tests, with the Bonferroni correction applied to prevent spurious results due to the multiple comparisons. All results stated as being significant are at the 0.05 confidence level, after the Bonferroni correction.

Results

Fit of the path

The goodness of the fits of the three models to the experimentally recorded data, in terms of the error measures defined in Eq. 14, are summarized in Table 1.

In terms of the path error E_{xy}, the best model (minimum angular jerk) predicts the path well with a small average error (<1 mm), while for some subjects the inertia-like cost and the minimum torque-change models are an order of magnitude worse than the minimum angular jerk model. Smaller differences between the models are observed in the velocity error E_{vel}. The posture errors E_{posture} show relatively larger errors (compared to the magnitudes of the movements) than for the other measures.

The following results refer to comparisons using multiple t tests, after taking into account the Bonferroni correction. For the path (E_{xy}) and posture (E_{posture}) errors, the minimum angular jerk had significantly lower errors than the inertia-like cost model, which in turn had significantly lower errors than the minimum torque-change model. For the velocity (E_{vel}) error, there were no significant differences between the minimum angular jerk and the inertia-like models, but both these models had significantly lower errors than the minimum torque-change model.

Four typical movements for Subject 2 are presented in Fig. 1. This figure shows the fit to the path, and the three joint angles. Figure 2 presents the torque predictions for the three joints, where the torque was calculated using Eq. 10.

From Fig. 1, it can be observed that for the path, the minimum torque-change model generally predicted a path with curvature opposite to that observed in the other models. In terms of the joint angles, it can be observed that the medial phalange moves more than the other phalanges of the finger. The shape of the joint angles' trajectories were similar (although scaled) between the different movements and joints.

In Fig. 2, where the torque is plotted for the different models, the models produce predictions of joint torque that are qualitatively similar to the experimental data.

In the second set of experiments, a weight of 20 g was added to the medial phalange. Over the duration of the experiment (approximately 30 min), learning effects were not observed, that is, similar trajectories were observed at the beginning and end of the recording session. The shape of the fingertip paths were very similar to those seen when the subjects were not wearing the lead spiral. Figure 3 contrasts the different predictions for a typical movement with and without the added weight. When the weight

Table 1 The goodness of the fit for the three models—minimum inertia-like cost, minimum torque change model and minimum angular jerk model

Subject	Error measure	Inertia-like cost	Minimum torque change	Minimum angular jerk
1	$E_{xy}(\times 10^{-4})$	17.25(±21.89)	58.77(±67.67)	9.58(±19.88)
	$E_{vel}(\times 0.01)$	2.62(±2.60)	4.00(±3.45)	2.53(±2.76)
$n = 34$	$E_{\theta}(\times 0.1)$	18.71(±10.86)	47.53(±25.08)	8.30(±6.38)
2	$E_{xy}(\times 10^{-4})$	13.71(±10.93)	60.06(±55.62)	8.40(±8.20)
	$E_{vel}(\times 0.01)$	2.61(±1.75)	3.84(±2.89)	2.64(±1.82)
$n = 38$	$E_{\theta}(\times 0.1)$	14.28(±6.01)	47.24(±21.48)	9.29(±4.56)
3	$E_{xy}(\times 10^{-4})$	6.58(±5.59)	25.27(±26.58)	3.46(±3.94)
	$E_{vel}(\times 0.01)$	2.21(±1.40)	2.47(±1.75)	2.27(±1.41)
$n = 22$	$E_{\theta}(\times 0.1)$	7.76(±4.13)	20.02(±5.59)	5.06(±2.97)
4	$E_{xy}(\times 10^{-4})$	9.12(±10.70)	24.86(±28.76)	5.53(±10.51)
	$E_{vel}(\times 0.01)$	3.07(±1.66)	4.02(±1.96)	2.89(±1.87)
$n = 23$	$E_{\theta}(\times 0.1)$	11.99(±5.20)	24.60(±11.07)	5.75(±5.28)

The units for the path errors E_{xy} are m, for velocity errors E_{vel} are m s^{-1}, and for posture $E_{posture}$ are radians

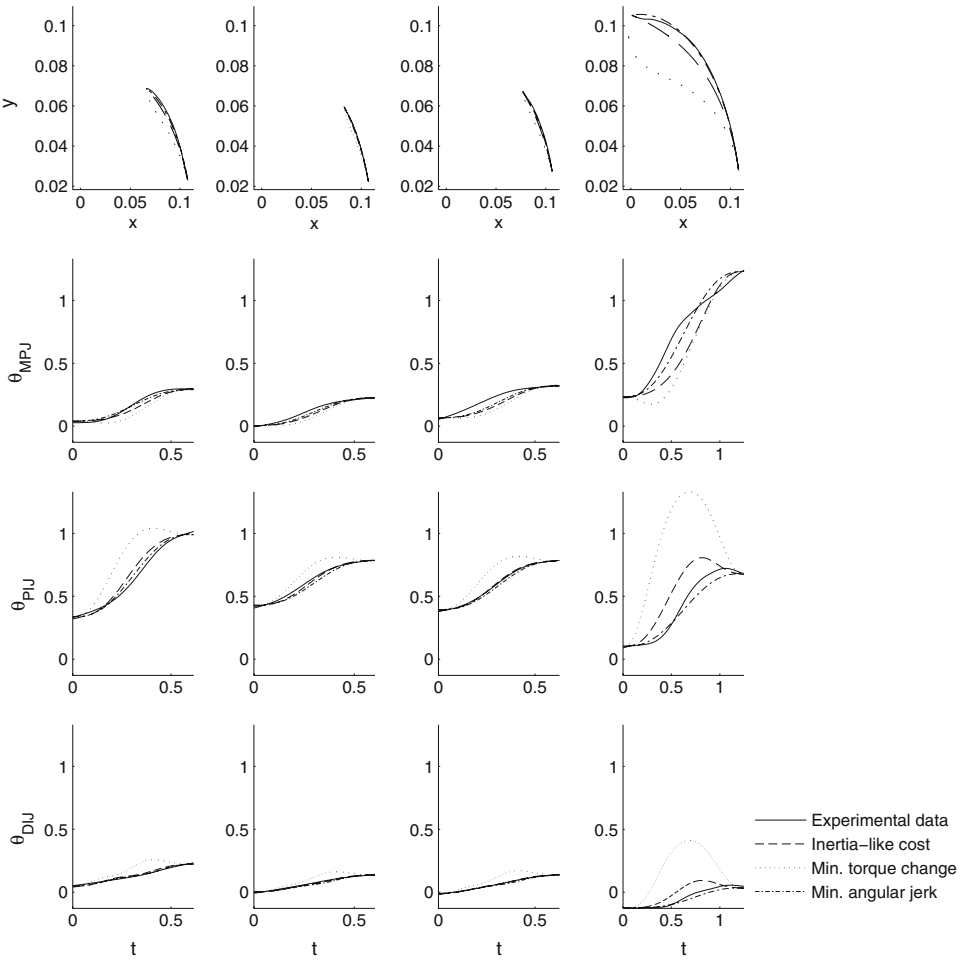

Fig. 1 Experimental data and model predictions for four typical movements for Subject 2. Along with the experimental data, the predictions are shown for the minimum weighted squared joint derivatives (inertia-like cost), minimum torque-change model and the minimum angular jerk model. The *first row* is in Cartesian space (x vs. y), in m, the *next three rows* are the joint angles (in radians) plotted against time (s). Each column is a different movement

is added, the inertia-like cost prediction becomes more straight, and the minimum torque change prediction becomes much more curved.

The fits of the model when a weight of 20 g was added to the medial phalange are presented in Table 2.

Four typical movements for Subject 2 are presented for the endpoint and joint angles in Fig. 4 and the joint torques in Fig. 5 for the condition with the added weight.

With the added weight, the multiple t tests gave the same conclusions as without the added weight. When

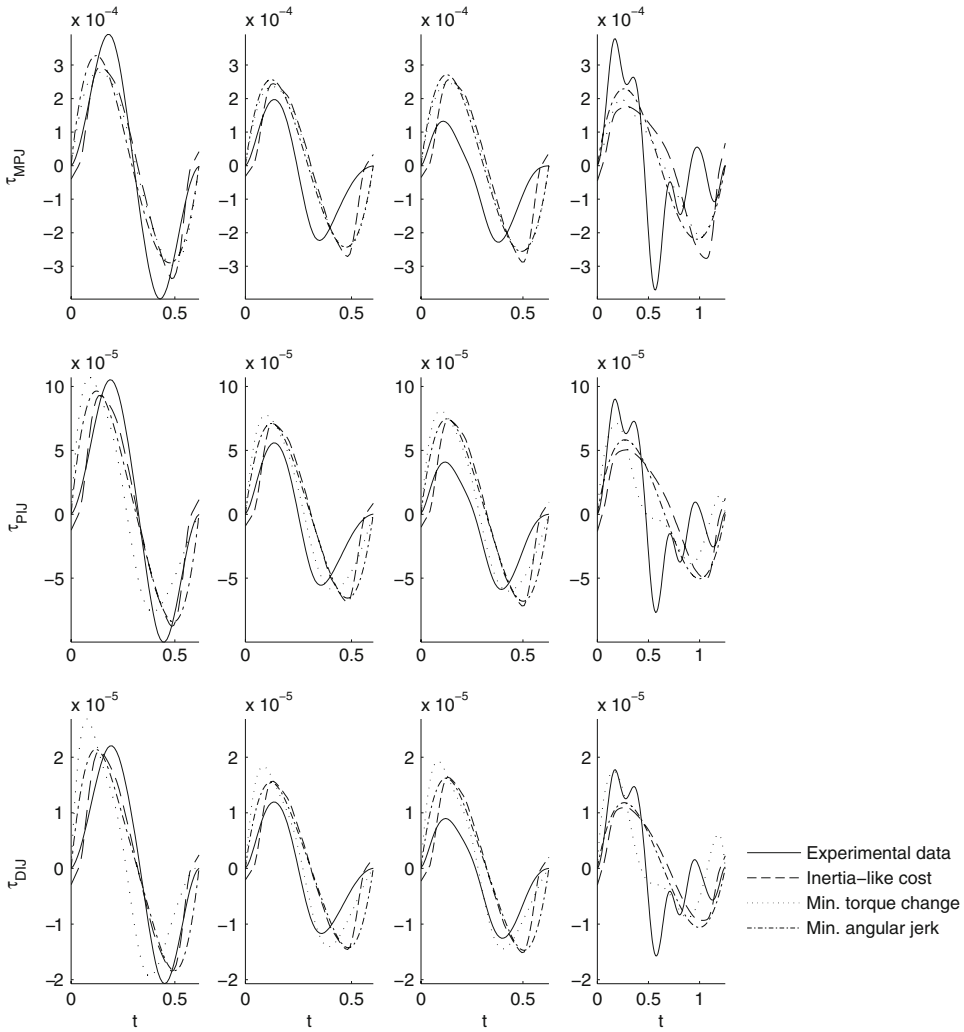

Fig. 2 Model predictions in terms of torque (N m) for the three joints for the four movements plotted in Fig. 1. The models are as described in Fig. 1. *Each row* is the torque at one joint, and *each column* is a different movement

comparing the predictions of the same model between the initial experiments and the experiments with the added weight, the quality of fit of the predictions was significantly worse for the torque-change model with all error measures, but no significant differences were observed with the other two models.

Sensitivity of model predictions to variations in parameters

The phalange lengths, phalange radii, center of mass of the phalanges and the density of the finger are all used in the calculation of the inertia matrix. The sensitivity of the calculated errors to variations in these parameters was quantified by systematically varying each parameter, re-performing the optimization, and calculating the errors (as defined in Eq. 14). The average errors were calculated for the inertia-like model, and the minimum torque-change model, because only these two models were dependent on the inertia matrix. The results of varying the parameters for Subject 1 can be found in Figs. 6 and 7. Even with these variations to the models, the statistical conclusions presented above are unchanged.

Discussion

During grasping movements, the fingers have been observed to show stereotypical trajectories. In particular, the path of the fingertip was observed to be well described by a logarithmic spiral (Kamper et al. 2003). While this provides a succinct description of the experimental observations, it does not provide a mechanism for the generation of these trajectories. In this work, three different optimization-based models were compared for their ability to describe the observed paths and joint angle trajectories, with the assumption that these are potential strategies that the CNS could use for planning finger movements during grasping. Based on the different error measures considered, given the initial and final postures of the finger, the minimum angular jerk model predicted well the observed trajectories, and this prediction was significantly better than

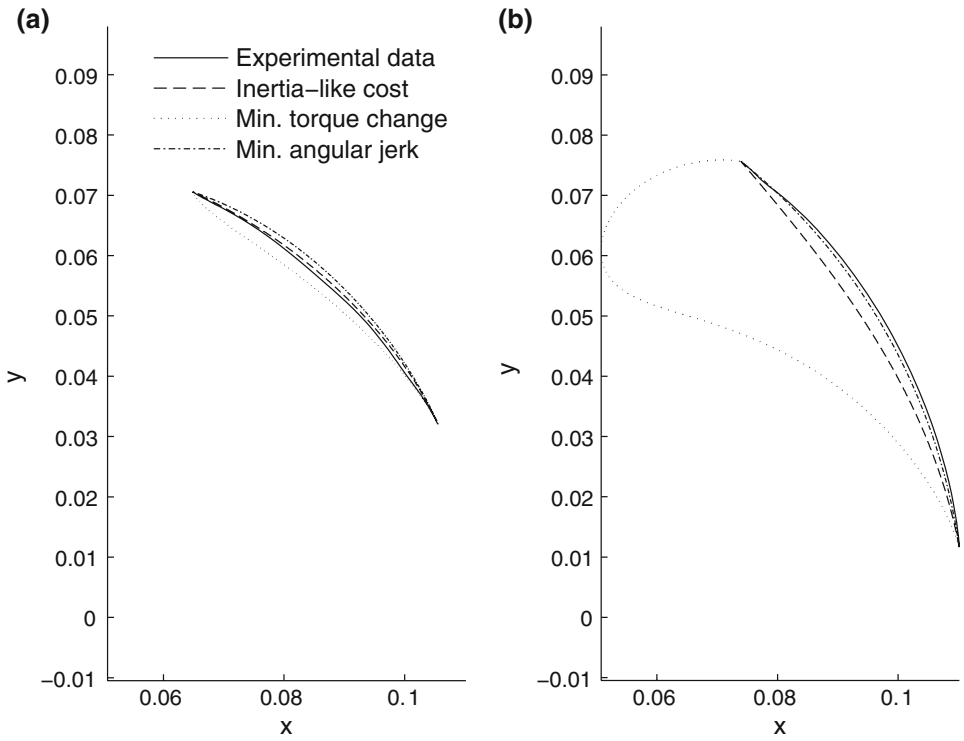

Fig. 3 Comparison of a typical movement (**a**) without and (**b**) with the added weight. Note that the path predicted by the inertia-like cost becomes more like a straight line, while the path predicted by the minimum torque-change model becomes much more curved, in the wrong direction

the other models considered. Flanagan and Ostry (1989) had found that a minimum angular jerk criterion modeled well vertical arm movements. In Laczko et al. (2000), it was observed that for arm movements, the jerk-related terms at the joint level dominate the endpoint jerk of the arm, and so minimization of endpoint jerk can be well approximated by minimization of joint jerk-related cost. Based on the results found in this work, our initial prediction that an inertia-like cost would best predict finger movements, as was found recently for arm movements (Biess et al. 2007) was not supported. Rather, probably due to the large differences in the physical properties and the inertia between the fingers and the arm, it appears that the CNS uses different strategies for the arm versus the fingers. Minimization of the angular jerk ensures smooth finger trajectories. These may be beneficial for finger movements during grasping, because they ensure that during the grasping of an object, the fingers will be moving slowly at the end of the movement, allowing time for corrections as the object is grasped.

The original formulation of the minimum jerk model (Flash and Hogan 1985), proposed for arm movements, predicts straight line paths of the end effector, and so is unsuitable for the curved paths observed for the fingers during grasping. While the model of Smeets and Brenner (1999) is able to produce curved trajectories by relaxing the requirement that the endpoint acceleration be zero, Kamper et al. (2003) have shown that this model is unsuitable for finger trajectories during grasping, due to its inability to reproduce the velocity profiles experimentally found. Furthermore, for the data recorded in our study, the endpoint accelerations of the fingers were observed to be zero at the endpoints.

Table 2 The goodness of fit for the three models with the added 20 g weight on the medial phalange, as described in Table 1

Subject	Error Measure	Inertia-like Cost	Minimum Torque change	Minimum Angular jerk
1	$E_{xy}(\times 10^{-4})$	19.76(±23.48)	77.23(±77.13)	5.78(±17.14)
	$E_{vel}(\times 0.01)$	5.05(±5.09)	6.31(±4.04)	5.36(±5.23)
$n = 19$	$E_{\theta}(\times 0.1)$	19.46(±10.69)	42.82(±15.94)	8.18(±8.23)
2	$E_{xy}(\times 10^{-4})$	15.21(±11.33)	120.29(±72.33)	8.95(±9.88)
	$E_{vel}(\times 0.01)$	2.74(±1.26)	6.27(±2.71)	2.72(±1.28)
$n = 22$	$E_{\theta}(\times 0.1)$	10.49(±4.92)	51.20(±28.08)	6.39(±3.28)
3	$E_{xy}(\times 10^{-4})$	4.49(±2.62)	30.36(±31.18)	2.20(±1.67)
	$E_{vel}(\times 0.01)$	1.83(±0.90)	2.79(±1.63)	1.84(±1.02)
$n = 12$	$E_{\theta}(\times 0.1)$	3.75(±1.38)	11.68(±4.02)	2.10(±1.51)
4	$E_{xy}(\times 10^{-4})$	6.95(±12.34)	15.49(±16.00)	6.82(±12.39)
	$E_{vel}(\times 0.01)$	1.99(±1.18)	2.38(±1.23)	1.90(±1.27)
$n = 12$	$E_{\theta}(\times 0.1)$	2.70(±2.00)	10.37(±6.84)	2.36(±1.88)

The minimum angular jerk model implies that the trajectory is not planned in terms of the end-point movement, but rather in terms of joint angles. While the velocity can be arbitrarily scaled with movement duration, the temporal and spatial aspects are coupled in this model.

Furthermore, if each joint follows such a trajectory, this implies that the joint angles of the finger are linearly

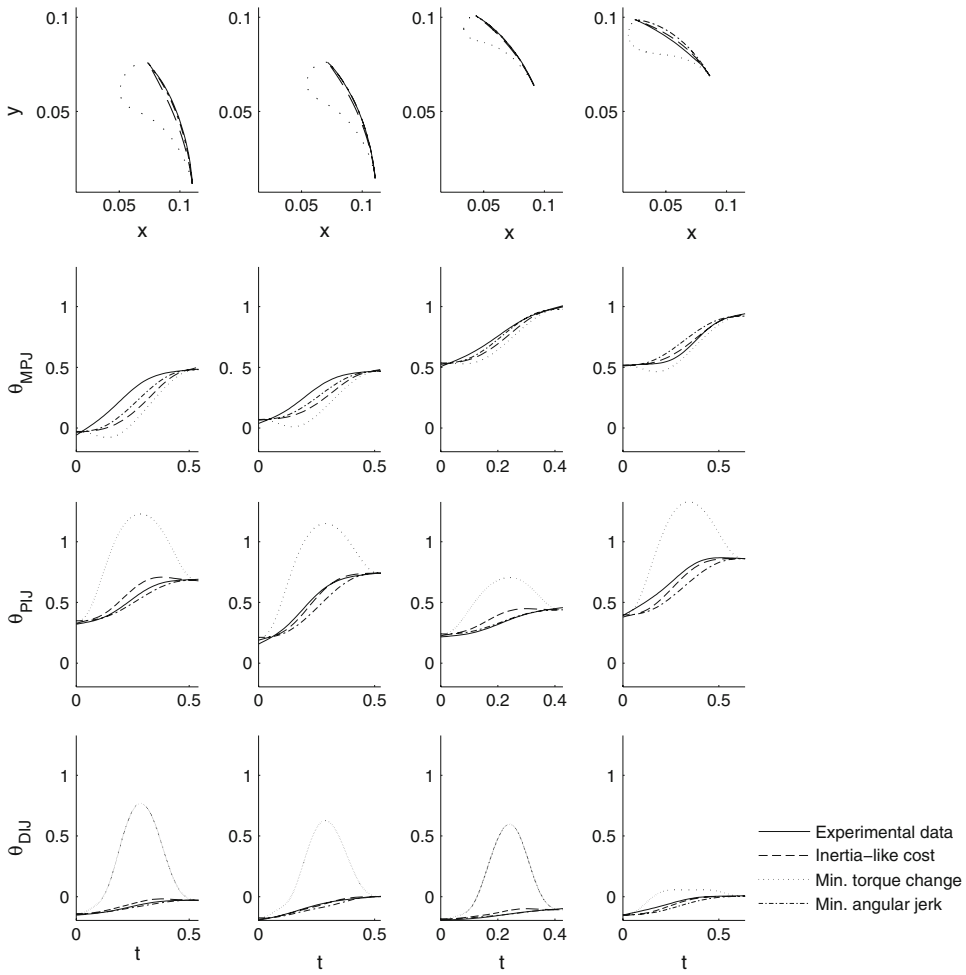

Fig. 4 The *xy* path and joint angle trajectories of the model and the experimental data for four typical movements for Subject 2, with the added 20 g weight on the medial phalange. The graphs are as described in Fig. 1

related, as was found in a recent study (Dejmal and Zacksenhouse 2006) examining manipulative movements on objects. This constant ratio between the joint velocities was first observed by Soechting and Lacquaniti (1981).

The coordinated action of the joints during grasping may be partially due to the biomechanics of the fingers. The extrinsic muscles flexor digitorum superficialis (FDS) and flexor digitorum profundus (FDP) contribute to finger flexion (Norkin and Levangie 1992). The FDP can flex the metacarpophalangeal, proximal interphalangeal and distal interphalangeal joints, and as was observed, this combined action may result in synchronizing motion at the three joints.

The joint trajectories observed showed that the medial phalange moved more than either the proximal or distal phalanges. While the use of a model based on minimizing a kinetic energy-related cost was found to predict less well the finger movements than other models, the minimum angular jerk model does not predict which posture should be used for a given endpoint, and hence energetic factors may be partially responsible for the selection of the endpoint posture. Accelerating the lighter medial phalange requires less torque than accelerating the proximal phalange (which also must rotate the other phalanges with it). The reason that the distal phalange, which weighs the least, and theoretically would not require rotating the other phalanges is not rotated more seems to be due to biomechanical constraints (Hahn et al. 1995). This biomechanical constraint was implemented in the models, and was needed in order to produce models with reasonable fits to the data.

The minimum torque-change model was found, in general, to predict the path and trajectories significantly worse than the other models. It predicted fingertip paths with a curvature opposite to that observed in the experimental data.

The poorer fit to the experimental data of the inertia-like model, and the minimum torque-change model were likely not due to errors in the inertia matrix, as systematic variation of these parameters did not improve significantly the fit of these models to the data.

When the inertia of the medial phalange was changed by adding a weight, the kinematics (i.e., the joint angle trajectories and the fingertip path) did not change significantly. In the minimum torque-change model, when the weight was added, the predictions became worse. The

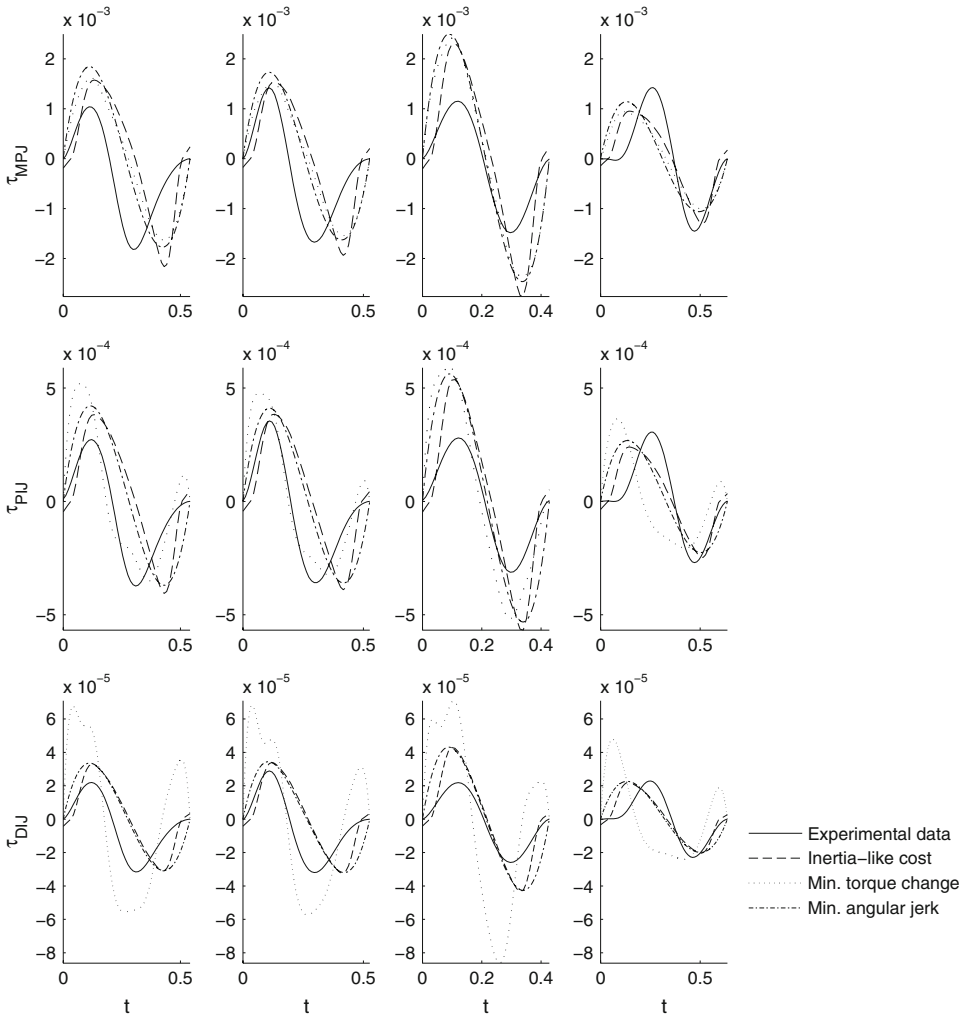

Fig. 5 Fits of the model in terms of torque with the added 20 g weight on the medial phalange for four typical movements for Subject 2. The graphs are as described in Fig. 1

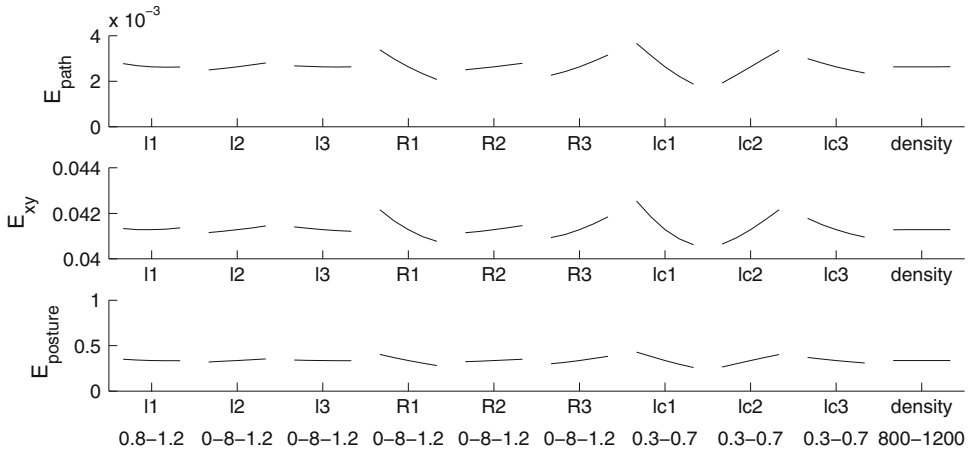

Fig. 6 Results of the sensitivity analysis for Subject 1, for the inertia-like model. The *graphs* show the average error, using the measures defined in Eq. 14, as a result of changing the model parameters, over the ranges shown. The phalange lengths, l_1, l_2 and l_3, the phalange radii R_1, R_2 and R_3, and the center of mass of the phalange, l_{c1}, l_{c2} and l_{c3} are lengths relative to the subject-dependent lengths used in the previously described models. The units of density are kg m^{-3}. None of the changes in the errors due to these changes in the parameters changed the conclusions described

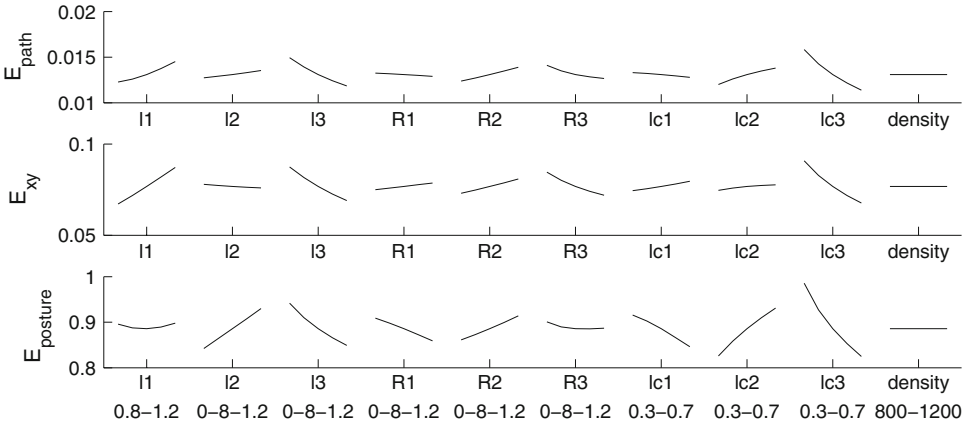

Fig. 7 Results of the sensitivity analysis for Subject 1, for the minimum torque-change model. The explanation of the graphs is the same as for Fig. 6

predicted paths become more curved, generally in the wrong direction. Even without the addition of the weight, the predicted trajectories were more curved than the observed trajectories, due to the medial and distal joint angles exceeding the final joint angles, and then returning. When the weight was added, the effect became larger.

Hence, there seems to be little support for using the inertia-like and minimum torque-change models in predicting index finger motion during grasping. In Biess et al. (2007) for arm movements, the inertia-like cost model was shown to model well arm movements. The difference in the findings may be explained by the different role that inertia plays in arm movements, where energetic considerations are important, and finger movements which have very low inertia and other factors may be more important in planning movements. It may also have been that with long-term adaptation, the trajectories may change to reflect the changes in the inertia; however, we do expect this to be the case.

The nature of the minimum angular jerk model is that its predictions do not depend upon the inertial properties of the finger, and thus did not change when a weight was added to the medial phalange. The large changes in the predictions of the minimum torque-change model, which is dependent on the finger inertial properties, with the change in weight of the medial phalange, that were not observed in the recorded finger movements, suggests that finger trajectories are in general not mainly dictated by dynamic criteria related to impedance. Nevertheless, it is possible that the characteristics of the trajectories could alternatively be modeled by taking into account the inertial properties of the fingers and the visco-elastic properties of the muscles and tendons, and could be modeled by a model that assumes two separate levels of trajectory planning and motor execution (Flash 1987) or a separation of planning of trajectory and final position (Scheidt and Ghez 2007), but this goes beyond the scope of the current study.

The different models have different numbers of free parameters. The inertia-like cost model has three parameters (the weights of the Jacobi polynomials) for each of the two joint angles which are fitted according to the cost function. However, these are not free parameters, rather, they enable the approximate minimization of the cost function, and are selected based on the cost function and not derived from the observed trajectories. Where analytic solutions to the minimization problem possible, then no parameters would have been required. A similar statement is true for the minimum torque-change model. Finally, the minimum angular jerk model does not have any parameters that need to be fitted since the analytic solution is known.

An apparent contradiction is observed between the finding that the path is well fitted by a logarithmic spiral, and the finding that the joint angle trajectories are linearly related, as these both cannot be true simultaneously (Friedman 2007). While mathematically this statement is true, based on the results in this paper, it is noted that the predictions of the minimum angular jerk model, at least for the trajectories studied in this work, are very close to logarithmic spirals, although this may not be true for other movements. It should be noted that while logarithmic spirals approximate reasonably well the finger path during grasping movements, they cannot describe general finger movements. For example, a radial movement of the finger performed, cannot be approximated by any logarithmic spiral. In Cruz and Kamper (2006), where subjects were asked to make point-to-point finger movements in the plane, the observed trajectories could not be well fitted by logarithmic spirals. Use of the models presented in this work for such trajectories would serve as a good test for their generalization to more general finger movements, rather than to the specific finger movements involved in grasping, although more complex movements may involve the composition of multiple sub-movements. The examination of tasks requiring particular force and/or velocity demands, for example, playing the piano, using tools, or manipulating an object, could also help determine the general applicability of such models.

The stereotypical trajectories observed in this work are based on more than simply biomechanical constraints. This

can be deduced from observations of patients that cannot balance the activation of their intrinsic and extrinsic muscles, who do not generate these stereotypical trajectories (Littler 1973).

Acknowledgments This research was supported in part by the German–Israeli Project Cooperation (DIP) and by the Moross Laboratory at the Weizmann Institute of Science. Tamar Flash is an incumbent of the Dr. Hymie Morros Professorial chair. We thank Armin Biess for his assistance in generating the predicted trajectories.

Appendix: dynamic equations

Complete details of the derivation can be found in Friedman (2007). The 3 × 3 inertia matrix for a 3 joint finger is given by

$$\begin{aligned}
M_{1,1} &= (2lc_3c_3l_2 + l_2^2 + l_1^2 + 2lc_3l_1c_{23} + lc_3^2 + 2l_2l_1c_2)m_3 \\
&\quad + m_1lc_1^2 + I_{z1} + I_{z2} + I_{z3} + 2m_2c_2l_1lc_2 \\
&\quad + m_2lc_2^2 + l_1^2m_2 \\
M_{1,2} &= (l_2^2 + lc_3^2 + 2lc_3c_3l_2 + lc_3l_1c_{23} + l_2l_1c_2)m_3 \\
&\quad + m_2c_2l_1lc_2 + m_2lc_2^2 + I_{z2} + I_{z3} \\
M_{1,3} &= (lc_3 + c_3l_2 + l_1c_{23})m_3lc_3 + I_{z3} \\
M_{2,2} &= (l_2^2 + lc_3^2 + 2lc_3c_3l_2)m_3 + m_2lc_2^2 + I_{z2} + I_{z3} \\
M_{2,3} &= (lc_3 + c_3l_2)m_3lc_3 + I_{z3} \\
M_{3,3} &= m_3lc_3^2 + I_{z3}
\end{aligned} \tag{15}$$

where l are the lengths of the phalanges, lc are the lengths to the center of the phalanges, c_i is the cosine of joint angle i, c_{ij} is the cosine of angle $i + j$, s_i is the sine of joint angle i, and m are the masses of the phalanges.

The other three terms of the inertia matrix can be found from the symmetry property of the inertia matrix.

The Coriolis and centrifugal forces are given by

$$\begin{aligned}
C_{1,1} &= -\dot{\theta}_2l_1(m_2s_2lc_2 + m_3l_2s_2 + m_3s_{23}lc_3) \\
&\quad - \dot{\theta}_3m_3(lc_3s_3l_2 + l_1s_{23}lc_3) \\
C_{1,2} &= -\dot{\theta}_1l_1(s_2m_2lc_2 + m_3l_2s_2 + s_{23}m_3lc_3) \\
&\quad - \dot{\theta}_2l_1(m_2s_2lc_2 + m_3l_2s_2 + m_3s_{23}lc_3) \\
&\quad - \dot{\theta}_3m_3(s_3l_2lc_3 + l_1s_{23}lc_3) \\
C_{1,3} &= -m_3lc_3(\dot{\theta}_1 + \dot{\theta}_2 + \dot{\theta}_3)(s_3l_2 + l_1s_{23}) \\
C_{2,1} &= \dot{\theta}_1(m_2s_2l_1lc_2 + m_3l_1l_2s_2 + l_1s_{23}m_3lc_3) \\
&\quad - \dot{\theta}_3(m_3s_3l_2lc_3) \\
C_{2,2} &= -\dot{\theta}_3m_3s_3l_2lc_3 \\
C_{2,3} &= -m_3s_3l_2lc_3(\dot{\theta}_1 + \dot{\theta}_2 + \dot{\theta}_3) \\
C_{3,1} &= m_3lc_3(\dot{\theta}_1s_3l_2 + \dot{\theta}_1l_1s_{23} + \dot{\theta}_2s_3l_2) \\
C_{3,2} &= m_3s_3l_2lc_3(\dot{\theta}_1 + \dot{\theta}_2) \\
C_{3,3} &= 0
\end{aligned}$$

References

Berkinblit M, Gelfand I, Feldman A (1986) Model of the control of the movements of a multijoint limb. Biophysics 31:142–153

Biess A, Nagurka M, Flash T (2006) Simulating discrete and rhythmic multi-joint human arm movements by optimization of nonlinear performance indices. Biol Cybern 95:31–53

Biess A, Liebermann D, Flash T (2007) A computational model for redundant human three-dimensional pointing movements: integration of independent spatial and temporal motor plans simplifies movement dynamics. J Neurosci 27:13045–13064

Cruz E, Kamper D (2006) Kinematics of point-to-point finger movements. Exp Brain Res 174:29–34

Dejmal I, Zacksenhouse M (2006) Coordinative structure of manipulative hand-movements facilitates their recognition. IEEE Trans Biomed Eng 53:2455–2463

Dempster W (1955) Space requirements of the seated operator. Technical Report WADC-TR-55-159, Aerospace Medical Research Laboratories, Wright-Patterson Air Force Base, OH

Flanagan J, Ostry D (1989) Trajectories of human multi-joint arm movements: evidence of joint level planning. In: Hayward V, Khatib O (eds) Experimental robotics I. Lecture Notes in Control and Information Sciences. Springer, Germany, pp 594–613

Flash T (1987) The control of hand equilibrium trajectories in multi-joint arm movements. Biol Cybern 57:257–274

Flash T, Hogan N (1985) The coordination of arm movements: an experimentally confirmed mathematical model. J Neurosci 5:1688–1703

Friedman J (2007) Features of human grasping. PhD thesis, Weizmann Institute of Science, Israel

Friedman J, Flash T (2007) Task-dependent selection of grasp kinematics and stiffness in human object manipulation. Cortex 43:444–460

Gupta A, Rash GS, Somia NN, Wachowiak MP, Jones J, Desoky A (1998) The motion path of the digits. J Hand Surg 23A:1038–1042

Hahn P, Krimmer H, Hradetzky A, Lanz U (1995) Quantitative analysis of the linkage between the interphalangeal joints of the index finger. J Hand Surg 20B:696–699

Hermens F, Gielen S (2004) Posture-based or trajectory-based movement planning: a comparison of direct and indirect pointing movements. Exp Brain Res 159:340–348

Jeannerod M (1981) Intersegmental coordination during reaching at natural visual objects. In: Long J, Baddeley A (eds) Attention and performance IX, Lawrence Erlbaum Associates, Philadelphia, pp 153–169

Kamper D, Cruz E, Siegel M (2003) Stereotypical fingertip trajectories during grasp. J Neurophysiol 90:3702–3710

Laczko J, Jaric S, Tihanyi J, Zatsiorsky V, Latash M (2000) Components of the end-effector jerk during voluntary arm movements. J Appl Biomech 16:14–25

Littler JW (1973) On the adaptability of man's hand (with reference to the equiangular curve). Hand 5:187–191

Mason C, Gomez J, Ebner T (2001) Hand synergies during reach-to-grasp. J Neurophysiol 86:2896–2910

Murray R, Li Z, Sastry S (1994) A mathematical introduction to robotic manipulation. CRC Press, Boca Raton

Nakano E, Imamizu H, Osu R, Uno Y, Gomi H, Yoshioka T, Kawato M (1999) Quantitative examinations of internal representations for arm trajectory planning: minimum commanded torque change model. J Neurophysiol 81:2140–2155

Norkin CC, Levangie PK (1992) Joint structure and function. A comprehensive analysis, 2nd edn. F.A. Davis Company, Philadelphia

Okadome T, Honda M (1999) Kinematic construction of the trajectory of sequential arm movements. Biol Cybern 80:157–169

Rosenbaum D, Meulenbroek R, Vaughan J, Jansen C (2001) Posture-based motion planning: applications to grasping. Psychol Rev 108:709–734

Santello M, Flanders M, Soechting J (2002) Patterns of hand motion during grasping and the influence of sensory guidance. J Neurosci 22:1426–1435

Scheidt RA, Ghez C (2007) Separate adaptive mechanisms for controlling trajectory and final position in reaching. J Neurophysiol 98:3600–3613

Secco E, Visiolo A, Magenes G (2004) Minimum jerk motion planning for a prosthetic finger. J Robotic Syst 21:361–368

Smeets J, Brenner E (1999) A new view on grasping. Motor Control 3:237–271

Soechting J, Lacquaniti F (1981) Invariant characteristics of a pointing movement in man. J Neurosci 1:710–720

Soechting J, Buneo C, Herrmann U, Flanders M (1995) Moving effortlessly in three dimensions: does Donder's law apply to arm movement? J Neurosci 15:6271–6290

Uno Y, Kawato M, Suzuki R (1989) Formation and control of optimal trajectory in human multijoint arm movement. Biol Cybern 61:89–101

Wada Y, Kaneko Y, Nakano E, Osu R, Kawato M (2001) Quantitative examinations for multi joint arm trajectory planning—using a robust calculation algorithm of the minimum commanded torque change trajectory. Neural Netw 14:381–393